

# Molecular Gas Heating and Modified Dust Properties in Active Galaxies: Growing Black Holes or Tidal Shocks?

REBECCA MINSLEY,<sup>1</sup> ANDREEA PETRIC,<sup>2,3</sup> ERINI LAMBRIDES,<sup>4</sup> ALEKSANDAR M. DIAMOND-STANIC,<sup>1</sup> MAYA MERHI,<sup>5</sup>  
MARCO CHIABERGE,<sup>6</sup> AND NICOLAS FLAGEY<sup>3</sup>

<sup>1</sup>*Department of Physics and Astronomy, Bates College, 44 Campus Avenue, Lewiston, ME 04240, USA*

<sup>2</sup>*Institute for Astronomy, 2680 Woodlawn Drive, Honolulu, HI, 96822, USA*

<sup>3</sup>*Canada-France-Hawaii Telescope, 65-1238 Mamalahoa Highway, Kamuela, HI, 96743, USA*

<sup>4</sup>*Department of Physics & Astronomy, Johns Hopkins University, Bloomberg Center, 3400 N. Charles St., Baltimore, MD 21218, USA*

<sup>5</sup>*Lycoming College, 700 College Pl, Williamsport, PA 17701, USA*

<sup>6</sup>*Space Telescope Science Institute, 3700 San Martin Dr, Baltimore, MD 21218*

## ABSTRACT

We investigate if and how growing super-massive black holes (SMBH) known as Active Galactic Nuclei (AGN) and gravitational interactions affect the warm molecular gas and dust of galaxies. Our analysis focuses on the morphologies and warm ISM properties of 630 galaxies at  $z < 0.1$ . We use *grizy* images from the Pan-STARRS survey to classify the galaxies into mergers, early mergers, and non-mergers. We use MIR spectroscopic measurements of emission from rotational  $H_2$  transitions, dust and PAH features, and silicate emission or absorption lines at  $9.7 \mu\text{m}$  to study how gravitational interactions impact the warm ISM in AGN and non-AGN hosts.

We find that in AGN-hosts, the ISM is warmer, the ratios of  $H_2$  to PAHs are larger, the PAH emission line ratios and silicate strengths have a wider range of values than in non-AGN hosts. We find some statistical differences between the  $H_2$  emission of mergers and non-mergers, but those differences are less statistically significant than those between AGN and non-AGN hosts.

Our results do not establish a relation between the rate of BH growth and the warm ISM but point to highly statistically significant differences between AGN hosts and non-AGN hosts, differences that are not present with the same statistical significance between mergers and non-mergers. We speculate that the combination of triggering mechanisms, AGN orientations, and evolutionary stages that allow AGN to be classified as such in the MIR indicate that those AGN are energetically coupled on kpc scales to their host galaxies's warm ISM. Future optical and IR, spatially resolved spectroscopic studies are best suited to characterize this connection.

## 1. INTRODUCTION

Growing super-massive black holes (SMBH) power compact, luminous, galactic centers known as Active Galactic Nuclei (AGN). At low redshifts, the most luminous AGN appear to be triggered by galaxy mergers (Ellison et al. 2019). The changing gravitational potential of merging galaxies may allow a fraction of the gas to lose angular momentum and fall toward the center of the galaxy where it can feed any present SMBH or get compressed and induce star-formation (Hopkins et al. 2007, 2016). In this scenario some of the massive stars produced in the merger and the growing SMBH consume the surrounding ISM and inject energy into it through shocks, radiation, and turbulence. These processes increase the pressure in the gas, ionize part of it, and ultimately impede star-formation and SMBH growth (Hopkins et al. 2007; Ellison et al. 2019). Several parts of this scenario have been tested but the connections between AGN and their hosts' molecular gas on kpc scale are unclear.

The ISM fuels the growth of stars and of SMBHs. The ISM is heated, ionized, and shocked by gravitational interactions, new stars, stellar deaths, and AGN winds, emission, and jets. Therefore, to understand a galaxy's evolution we need to study the amount, phase-structure, and temperature of its ISM.

Spectroscopic observations in the MIR are a powerful way to identify and characterize AGN and a fraction of their ISM because in the MIR the AGN emission is (almost) not affected by extinction. Furthermore, the sources of MIR emission (ionized interstellar gas, non-thermal radio sources, and dust particles) can be empirically separated through a multitude of diagnostics (e.g. Genzel et al. 1998; Rigopoulou et al. 2002; Armus et al. 2007; Díaz-Santos et al. 2010; Petric et al. 2011). The warm (200-1000 K) molecular gas observed in the MIR makes up about 1% to 30% of the total molecular  $H_2$  mass (Roussel et al. 2007). Studies of nearby radio galaxies (e.g. Ogle et al. 2007) and mergers

(Guillard et al. 2009) showed that the warm molecular gas properties (mass, temperature, total luminosity relative to other coolants) can be used to estimate if and how the total ISM is affected by an AGN and/or by shocks associated with gravitational interactions. Important mechanisms responsible for exciting the MIR  $\text{H}_2$  rotational transitions are: photoionization in star-forming regions (Gautier et al. 1976; Bally & Lane 1982), AGN activity, X-ray heating, fluorescence induced by a non-thermal ultraviolet continuum, and shock heating by radio jets (Moorwood & Oliva 1988; Larkin et al. 1998; Ogle et al. 2007; Guillard et al. 2012). Rotational  $\text{H}_2$  emission may also be powered by shocks in dense clumps of filaments associated with interacting galaxies (Appleton et al. 2006; Ogle et al. 2007; Guillard et al. 2009). Radio galaxies, some mergers, and some IR bright galaxies have enhanced  $\text{H}_2$  emission with respect to the other MIR cooling lines (e.g. PAH, [Si II]) which suggests that shocks associated with supernova remnants, AGN, or tidal interactions can contribute significantly to the excitation of the  $\text{H}_2$  rotational transitions (Hill & Zakamska 2014; Stierwalt et al. 2014; Petric et al. 2018; Lambrides et al. 2019).

Spatially resolved studies of radio jets environments in X-rays, radio, and molecular gas showed how jet-ISM interactions can propagate shocks into the ISM and affect star-formation (Lanz et al. 2015; Ogle et al. 2014; Appleton et al. 2018). In nearby Luminous Infrared Galaxies (LIRGS with  $L_{\text{IR}} > 10^{11} L_{\odot}$ ) about 20% of warm  $\text{H}_2$  heating may come from AGN, AGN hosts have warmer molecular gas than non-AGN hosts, and the sources with the biggest warm gas kinetic energies are mergers (Stierwalt et al. 2014; Petric et al. 2018). The results of Stierwalt et al. (2014); Petric et al. (2018) were based on relatively small numbers of AGN which made it difficult to compare AGN merger hosts to AGN non-merger hosts and SF merger hosts to SF non-merger hosts. More recently Lambrides et al. (2019) compiled  $\sim 2000$  MIR spectra taken by the Spitzer Space Telescopes (Werner et al. 2004) Infrared Spectrograph (IRS, Houck et al. 2004) and found a strong statistical trend for AGN hosts to have warmer (by  $\sim 200$  K) warm molecular gas than non-AGN hosts, based on the  $\text{H}_2$  S(5) - S(3) transitions. While it is clear that AGN host galaxies may have a warmer molecular gas component (Rigopoulou et al. 2002; Ogle et al. 2007; Zakamska 2010; Nesvadba et al. 2011; Hill & Zakamska 2014; Stierwalt et al. 2014; Petric et al. 2018; Lambrides et al. 2019), it is unclear what physical mechanism is responsible for heating up the molecular gas in most sources. Because the data we present lack both the spatial and spectral resolution to test the details of those physical mechanisms, in this paper, we limit our investigation to one question: can the higher temperatures measured by Lambrides et al. (2019) be associated with merging hosts and not driven by the presence of an AGN? To test this we study the morphologies of the  $z < 0.1$  galaxies in the Lambrides et al. (2019) and perform a complementary statistical analysis that includes non-detections. The answer to this is connected to a more physically interesting question: is it possible that the mechanisms which trigger AGN in mergers also heat up the gas, or do any AGN emissions, jets, winds, or outflows affect the temperature of the gas irrespective of the gravitational interactions of the host galaxies.

The remainder of this paper is organized as follows: in section 2 we present our sample of galaxies, the visual merger classification and the statistical tools we used to estimate the relative effect that mergers have on the temperature of the warm molecular ISM-component compared to AGNs. In section 3 we present our results for the warm molecular gas, the PAH size distribution and ionization, and the silicate strengths. In section 4 we discuss what our results may suggest about how galaxy interactions and growing SMBH impact the warm component of a galaxy's ISM. We adopt cosmological parameters of  $h = 0.7$ ,  $\Omega_m = 0.3$ ,  $\Omega_{\Lambda} = 0.7$ .

## 2. SAMPLE AND ANALYSIS

We classify a  $z < 0.1$  subsample of galaxies used in Lambrides et al. (2019) as mergers, early mergers, or non-mergers. We approximate the temperature of the warm molecular gas using the mid-infrared molecular emission lines of  $\text{H}_2$  S(3) and the  $\text{H}_2$  S(1). We use those temperatures together with the ratio of the  $\text{H}_2$  S(3) to the  $11.3 \mu\text{m}$  PAH to test if AGN and/or gravitational interactions affect the warm ISM. Roussel et al. (2007); Zakamska (2010); Petric et al. (2018); Lambrides et al. (2019) find that the molecular emission lines ratios  $\text{H}_2$  S(3) to  $\text{H}_2$  S(1) are not affected by extinction.

### 2.1. Targets

The 2,015 galaxies analyzed by Lambrides et al. (2019) have redshifts between  $z = 0.001$  and  $z = 4.27$  and were selected from the Spitzer archive<sup>1</sup> based on proposal topics related to active galaxies. The reduced spectra were provided by the Combined Atlas of Sources with Spitzer IRS Spectra (Lebouteiller et al. 2011, CASSIS), but further

<sup>1</sup> <https://sha.ipac.caltech.edu/applications/Spitzer/SHA/>

processed as described in Lambrides et al. (2019). Our morphology analysis (see section 2.3) is based on visual classification using Pan-STARRS images, and therefore our sample only includes the galaxies at  $z < 0.1$ ; given the typical spatial resolution of Pan-STARRS (0.7 - 0.8'') the visual classification becomes uncertain at higher redshifts (Nair & Abraham 2010).

While Lambrides et al. (2019) found no obvious, systematic effects on the dust/gas analysis associated with the heterogeneous nature of the sample, a significant number of radio-loud AGN would skew our analysis because radio-loud AGN are mostly hosted by mergers (Chiaberge et al. 2015). We use the FIRST survey catalog (Becker et al. 1994) to compute rest-frame 1.4 GHz luminosities, using a spectral index of -0.7 as in Lacy et al. (1993) and the radio-loud definition of Ivezić et al. (2002) to determine that only 10 galaxies in our sample are radio-loud AGN. We did the analysis with and without the 10 RL galaxies and found that they had a minimal impact on the statistical tests. A future paper on the entire sample of Lambrides et al. (2019) will employ higher image quality optical data to expand the analysis to the higher redshift sources in the sample and will also benefit from on-going radio surveys with which to investigate the connection between radio selected AGN and the warm molecular gas.

## 2.2. MIR measurements

Here we briefly present the MIR spectroscopic features used in our analysis. A more comprehensive description of those measurements is provided in Lambrides et al. (2019). We first assume the temperature of the warm molecular gas is proportional to the ratio of two emission lines from rotational transitions of  $H_2$ : S(3) (J=5-3 at  $9.665\mu m$ ) to S(1) (J=3-1 at  $17.035\mu m$ ). We then use the 6.2, 7.7, and  $11.3\mu m$  PAH features to study the impact AGN and mergers may have on the sizes and ionization states of the dust grains. The relative strength of the 6.2 to the 7.7 PAH bands changes with grain-size distribution while the ratio of the 11.3 to the 7.7 PAH complexes are a function of their ionization states (Li & Draine 2001; Draine & Li 2007). We use the strength of the  $9.7\mu m$  silicate feature as a proxy for dust obscuration. However, we note that differences in dust geometry relative to the sources of MIR emission may complicate the analysis (Zakamska 2010).

We use the intensity of the  $11.3\mu m$  PAH and its ratio to the  $24\mu m$  flux as an estimate of the importance of star-formation in the studied galaxies. We acknowledge the debate around the validity of using  $11.3\mu m$  PAH as a robust tracer of SFR in AGN hosts (Smith et al. 2007; Díaz-Santos et al. 2010; Diamond-Stanic & Rieke 2012).

The most direct methods employed to estimate the AGN contribution to the MIR emission in individual galaxies are the ratios of high to low ionization fine-structure emission lines. However, those lines require higher spectral resolution than that available to Lambrides et al. (2019). Diagnostics from the low-resolution data are based on the dust properties (e.g. PAH features and dust continuum emission). For large samples of sources, diagnostics based on the PAH ratios or the MIR continuum slope match those from high to low ionization lines ratios (Petric et al. 2011).

In figure 1 we present the cumulative distributions of the  $H_2$  S(3) to  $H_2$  S(1) ratios,  $H_2$  S(3) to  $11.3\mu m$  PAH flux ratios, the  $11.3\mu m$  to  $7.7\mu m$  PAHs emission ratios, and the silicate strengths.

The sample we present in this paper includes: 207 AGN (with  $6.2\mu m$  PAH EQW  $< 0.27\mu m$ ), 114 AGN+SF composites (with  $0.27 < 6.2\mu m$  PAH EQW  $< 0.54\mu m$ ), and 264 SF only galaxies (with  $6.2\mu m$  PAH EQW  $> 0.54\mu m$ ).

## 2.3. Visual Classification

Our visual classification attempts to identify all galaxies in our sample that show signs of gravitational disturbances. We classify our targets as either non mergers, early mergers, or mergers. While our visual classification techniques was based on that of Nair & Abraham (2010) we also referred to Larson et al. (2016); Stierwalt et al. (2013); Bridge et al. (2010); Zheng et al. (1997); Petric et al. (2011) for their investigations of morphologies of nearby galaxies. We define non mergers as galaxies without any visible signs of a gravitation disturbance. We categorize early mergers as galaxies that have an apparent neighbor galaxy within  $\sim 50$  kpc radius of its center.

Blumenthal et al. (2020) point out the difficulties in identifying early mergers: tidal features are more evident in high stellar mass objects, with a high-gas fraction, and are also dependent on the geometry of the merger and the viewing geometry. Therefore while we present some of the possible statistical differences between early mergers, mergers, and non-mergers, we focus on statistical differences between mergers and non-mergers. We postpone a more focused discussion about early mergers to an investigation using multiple classification techniques. We use the term *merger* to describe galaxies that show at least one of the following signatures of a gravitational disturbance: morphological asymmetries, tidal tails, shells, or multiple nuclei (see figure 2).

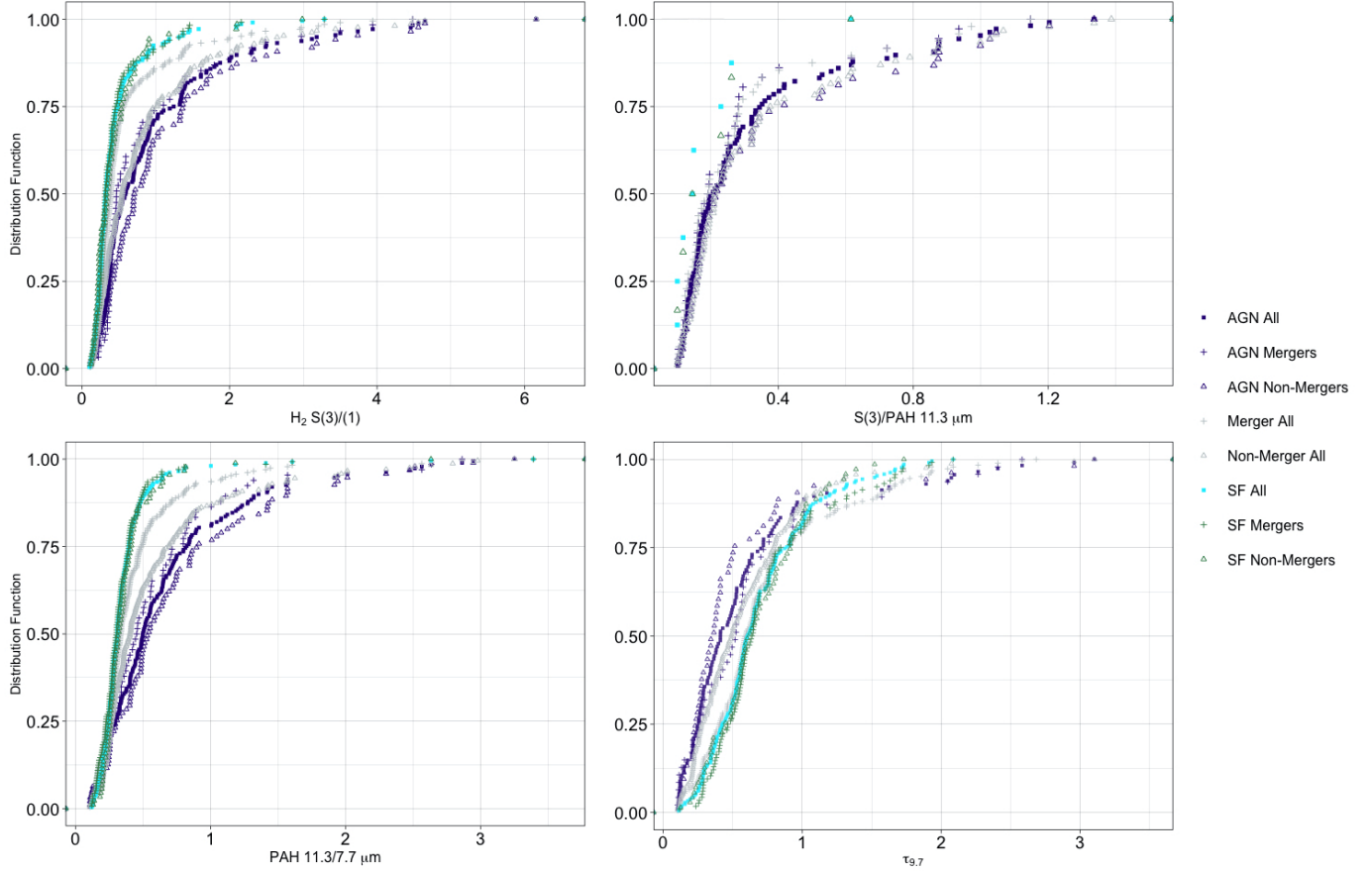


**Figure 1.** Cumulative distribution functions for of  $H_2$  S(3)/S(1) ratios (top left),  $H_2$  S(3)/11.3  $\mu m$  PAH ratios (top right), the 11.3  $\mu m$  PAH / 7.7  $\mu m$  PAH complex emission ratios (bottom left), and the silicate strengths  $\tau_{9.7\mu m}$  (bottom right).

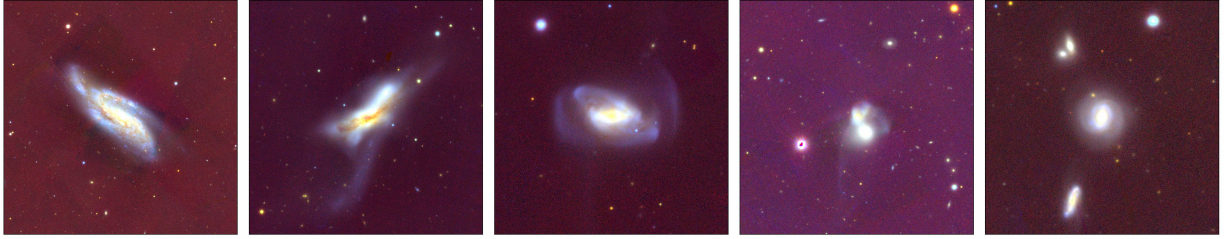


**Figure 2.** Pan-STARRS images of NGC 4088, NGC 0520, NGC 5218, NGC 4922 NED02, and UGC 07064 illustrating the different merger features we use for our classification: galaxy asymmetry, tidal tails, galactic shells, multiple nuclei and early/possible mergers for galaxies of similar brightness within 50 kpc of each-other.

We were unable to classify 45 galaxies due to either defects in the stacked multi-filter images or uncertainty in the morphological features indicating either a disturbance due to gravitational interactions or an intricate dust geometry. Excluding these 45 galaxies, the total number of galaxies in our sample is 585: 248 mergers, 257 non mergers and 80 early mergers. These results are summarized in Table 1 along with median values of the aforementioned MIR measurements. Three of the authors on this paper classified a subsample of 20 galaxies and were in excellent agreement: only two galaxies were assigned different classifications by one of the classifiers.

**Table 1.** Data Summary

|  | Merger | Non-Merger | Early Merger | Total |
|--|--------|------------|--------------|-------|
| Morphology classifications                               |        |            |              |       |
| AGN  | 73     | 104        | 30           | 207   |
| Star-forming   | 139    | 91         | 34           | 264   |
| AGN/SF   | 36     | 62         | 16           | 114   |
| Total  | 248    | 257        | 80           | 585   |
| Medians of H <sub>2</sub> S(3) to S(1) ratios            |        |            |              |       |
| AGN  | 0.5    | 0.7        | 0.3          | 0.6   |
| Star-forming   | 0.3    | 0.3        | 0.3          | 0.3   |
| For all above  | 0.4    | 0.5        | 0.3          | 0.4   |
| Medians of H <sub>2</sub> S(3) / 11.3 $\mu$ m PAH ratios |        |            |              |       |
| AGN  | 0.10   | 0.11       | 0.13         | 0.11  |
| Star-forming   | 0.01   | 0.01       | 0.01         | 0.01  |
| For all above  | 0.02   | 0.05       | 0.03         | 0.02  |
| Medians of 11.3 $\mu$ m PAH/ 7.7 $\mu$ m ratios          |        |            |              |       |
| AGN  | 0.4    | 0.5        | 0.4          | 0.5   |
| Star-forming   | 0.3    | 0.3        | 0.3          | 0.3   |
| For all above  | 0.3    | 0.4        | 0.3          | 0.3   |
| Medians of $\tau_{9.7\mu}$                               |        |            |              |       |
| AGN  | 0.3    | 0.2        | 0.1          | 0.2   |
| Star-forming   | 0.7    | 0.6        | 0.5          | 0.6   |
| For all above  | 0.6    | 0.3        | 0.3          | 0.5   |

### 3. RESULTS

#### 3.1. Statistical Analysis

We use the non-parametric, two sample tests, Logrank test and the Peto & Peto Generalized Wilcoxon test for censored data using the R statistical software package *survival* (Feigelson & Nelson 1985), to investigate the relative role of mergers and AGN on the warm molecular gas and dust. Those tests look at differences between reconstructed distributions of values derived from measurements of detected features and upper limits and a maximum-likelihood formalism developed by Kaplan & Meier (1958). This method was tested exhaustively by Isobe et al. (1986) using Monte-Carlo simulations.

In Table 2 we present the p-values from the Logrank, Peto, and Kolmogorov Smirnov (KS) tests which represent the likelihood that each of the two compared samples were drawn from a common population. The smaller the p-value the less alike the samples are. Values below 0.01 are significant, those between 0.01 and 0.1 are marginal and we only interpret them as possible hints for future analysis, values above 0.1 indicate no statistical differences between the samples compared, essentially telling us that the two populations are indistinguishable.

#### 3.2. Effects of a growing SMBH on the warm molecular gas and dust

We find that AGN hosts have higher H<sub>2</sub> S(3) to S(1) emission line ratios than non-AGN hosts suggesting higher molecular gas temperatures in AGN hosts. The median H<sub>2</sub> S(3) to H<sub>2</sub> (S1) ratio for all the AGN hosts is two times higher than that for SF hosts. We also find that AGN hosts have higher H<sub>2</sub> S(3) / 11.3  $\mu$ m PAH ratios than galaxies without an AGN which suggests that the observed warmer may be related to the AGN emission. The largest and most statistically significant differences in terms of H<sub>2</sub> temperatures and H<sub>2</sub> S(3) / 11.3  $\mu$ m PAH ratios are those between non-merger AGN hosts and non-merger SF hosts.

**Table 2.** A statistical table of warm ISM in active galaxies

| Comparison                          | H <sub>2</sub> S(3) / S(1)   | H <sub>2</sub> S(3) / PAH 11.3 $\mu$ m | PAH 6.2 $\mu$ m / PAH 7.7 $\mu$ m | PAH 11.3 $\mu$ m / PAH 7.7 $\mu$ m | PAH 11.3 $\mu$ m            | PAH 11.3 $\mu$ m / f <sub>24<math>\mu</math>m</sub> | $\tau_{9.7\mu\text{m}}$        |
|-------------------------------------|------------------------------|--|-----------------------------------|------------------------------------|-----------------------------|---|--------------------------------|
|                                     | Plog Ppeto <sup>a</sup>      | Plog Ppeto                             | Plog Ppeto                        | Plog Ppeto                         | Plog Ppeto                  | P <sub>KS</sub> Pwilcox                             |                                |
| Mergers vs. Non Mergers             | 2e-4 8e-5<br>(211 vs. 220)   | 7e-5 2e-5<br>(246 vs. 256)             | 0.3 0.3<br>(245 vs. 254)          | 4e-4 5e-4<br>(246 vs. 256)         | 0.1 0.1<br>(246 vs. 256)    | 0.02 0.04<br>(211 vs. 219)                          | 5e-06 3e-06<br>(214 vs. 230)   |
| AGN vs. SF                          | 4e-08 4e-09<br>(181 vs. 224) | <2e-16 <2e-16<br>(207 vs. 264)         | 2e-04 2e-04<br>(207 vs. 264)      | <2e-16 <2e-16<br>(207 vs. 264)     | 0.04 0.04<br>(207 vs. 264)  | 3e-08 3e-08<br>(180 vs. 224)                        | <2e-16 <2e-16<br>(185 vs. 230) |
| Mergers vs. Early Mergers           | 0.7 0.7<br>(211 vs. 71)      | 0.7 0.6<br>(246 vs. 80)                | 0.09 0.1<br>(245 vs. 78)          | 0.007 0.008<br>(246 vs. 80)        | 0.6 0.6<br>(246 vs. 80)     | 8e-04 0.002<br>(211 vs. 71)                         | 0.004 5e-04<br>(214 vs. 69)    |
| Non Mergers vs. Early Mergers       | 0.04 0.03<br>(220 vs. 71)    | 0.03 0.02<br>(254 vs. 78)              | 1.0 1.0<br>(256 vs. 80)           | 0.9 0.9<br>(256 vs. 80)            | 0.4 0.4<br>(219 vs. 71)     | 0.05 0.09<br>(230 vs. 69)                           | 0.9 0.8                        |
| Mergers – AGN vs. SF                | 0.02 0.01<br>(63 vs. 120)    | 6e-08 2e-08<br>(73 vs. 139)            | 0.05 0.05<br>(73 vs. 139)         | 2e-12 2e-12<br>(73 vs. 139)        | 0.4 0.4<br>(73 vs. 139)     | 3e-05 3e-05<br>(63 vs. 120)                         | 5e-06 7e-06<br>(64 vs. 121)    |
| Non Mergers – AGN vs SF             | 5e-06 2e-06<br>(89 vs. 75)   | 8e-09 7e-09<br>(104 vs. 91)            | 0.01 0.01<br>(104 vs. 91)         | 1e-08 9e-09<br>(104 vs. 91)        | 0.1 0.1<br>(104 vs. 91)     | 0.004 0.005<br>(88 vs. 75)                          | 1e-10 4e-10<br>(93 vs. 80)     |
| Early Mergers – AGN vs SF           | 0.1 0.1<br>(29 vs. 29)       | 0.01 0.008<br>(30 vs. 34)              | 0.1 0.1<br>(30 vs. 34)            | 8e-06 8e-06<br>(30 vs. 34)         | 8e-06 8e-06<br>(30 vs. 34)  | 0.04 0.04<br>(29 vs. 29)                            | 0.007 0.02<br>(28 vs. 29)      |
| AGN – Mergers vs. Non-Mergers       | 0.3 0.3<br>(63 vs. 89)       | 0.07 0.06<br>(73 vs. 104)              | 0.3 0.3<br>(73 vs. 104)           | 0.4 0.5<br>(73 vs. 104)            | 0.6 0.5<br>(73 vs. 104)     | 0.9 0.7<br>(63 vs. 88)                              | 0.005 0.01<br>(64 vs. 93)      |
| AGN – Mergers vs. Early-Mergers     | 0.4 0.3<br>(63 vs. 29)       | 0.7 0.7<br>(73 vs. 30)                 | 0.3 0.4<br>(73 vs. 30)            | 0.3 0.4<br>(73 vs. 30)             | 0.7 0.8<br>(73 vs. 30)      | 0.1 0.2<br>(63 vs. 29)                              | 0.4 0.2<br>(64 vs. 28)         |
| AGN – Non-Mergers vs. Early-Mergers | 0.02 0.01<br>(89 vs. 29)     | 0.1 0.1<br>(104 vs. 30)                | 0.9 0.9<br>(104 vs. 30)           | 0.6 0.7<br>(104 vs. 30)            | 0.6 0.6<br>(104 vs. 30)     | 0.02 0.05<br>(88 vs. 29)                            | 0.4 0.9<br>(93 vs. 28)         |
| SF – Mergers vs. Non-Mergers        | 0.9 0.9<br>(120 vs. 75)      | 0.9 0.9<br>(139 vs. 91)                | 0.7 0.8<br>(139 vs. 91)           | 0.2 0.2<br>(139 vs. 91)            | 0.001 5e-04<br>(139 vs. 91) | 0.2 0.2<br>(120 vs. 75)                             | 0.2 0.2<br>(121 vs. 80)        |
| SF – Mergers vs. Early Mergers      | 0.5 0.4<br>(120 vs. 29)      | 0.5 0.5<br>(139 vs. 34)                | 0.9 0.5<br>(139 vs. 34)           | 0.3 0.9<br>(139 vs. 34)            | 0.1 0.004<br>(139 vs. 34)   | 0.5 0.6<br>(120 vs. 29)                             | 0.004 0.007<br>(121 vs. 29)    |
| SF – Non-Mergers vs. Early Mergers  | 0.5 0.5<br>(89 vs. 29)       | 0.5 0.5<br>(139 vs. 34)                | 0.8 0.5<br>(91 vs. 34)            | 0.5 0.5<br>(91 vs. 34)             | 0.7 0.5<br>(91 vs. 34)      | 0.5 0.5<br>(75 vs. 29)                              | 0.04 0.1<br>(80 vs. 29)        |
| AGN/SF – Mergers vs. Non-Mergers    | 0.02 0.01<br>(28 vs. 56)     | 0.01 0.02<br>(28 vs. 56)               | 0.08 0.1<br>(33 vs. 59)           | 0.03 0.04<br>(34 vs. 61)           | 0.4 0.4<br>(34 vs. 61)      | 0.2 0.2<br>(28 vs. 56)                              | 0.3 0.2<br>(29 vs. 57)         |
| AGN/SF – Mergers vs. Early Merger   | 0.01 0.009<br>(28 vs. 13)    | 0.09 0.1<br>(28 vs. 13)                | 0.04 0.06<br>(33 vs. 14)          | 0.2 0.1<br>(34 vs. 16)             | 0.8 0.7<br>(34 vs. 16)      | 0.6 0.6<br>(28 vs. 13)                              | 0.4 0.2<br>(29 vs. 12)         |
| AGN/SF – Non vs. Early Merger       | 0.6 0.6<br>(56 vs. 13)       | 0.6 0.6<br>(56 vs. 13)                 | 0.4 0.4<br>(59 vs. 14)            | 0.6 0.7<br>(61 vs. 16)             | 0.6 0.6<br>(61 vs. 16)      | 0.8 0.8<br>(56 vs. 13)                              | 0.8 0.9<br>(57 vs. 12)         |

<sup>a</sup> The cited p-values from the logrank, peto, and Kolmogorov Smirnov (KS) tests give the likelihood that the two samples were drawn from a common population. As such, the smaller the p-value the less alike the samples are. Values below 0.01 are highly significant, those between 0.01 and below 0.1 are marginal and we only interpret them as possible hints for future analysis, values above 0.1 indicate the samples are drawn from the same population.



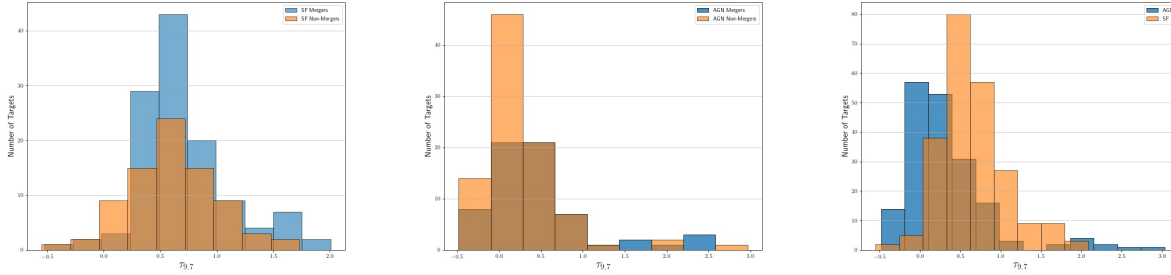


**Figure 3.** Histograms of silicate strengths measured by [Lambrides et al. \(2019\)](#) for: (left) SF merger and SF non-merger galaxies, (center) AGN host-mergers and non-mergers, and (right) all the AGN and all the non-AGN hosts in our sample.

The MIR emitting dust appears to also be affected by the presence of an AGN. We find statistically significant differences between the  $11.3 \mu\text{m}$  to  $7.7 \mu\text{m}$  PAHs emission ratios of AGN and non-AGN hosts with higher medians and a wider range of values for AGN hosts compared to non-AGN hosts. This result confirms, with a larger sample, the findings of [Smith et al. \(2007\)](#). [Smith et al. \(2007\)](#) suggest that this may be due to differences in the ionization states of the PAHs: the  $11.3 \mu\text{m}$  feature is thought to be produced by neutral PAHs, while the  $7.7 \mu\text{m}$  feature arises primarily from PAH cations (e.g. [Allamandola et al. 1999](#); [Draine & Li 2007](#)). As discussed in [Smith et al. \(2007\)](#) harder radiation fields destroy PAH grains, therefore, if the grain or molecular carriers of the  $7.7 \mu\text{m}$  PAH feature are not the same as those of the  $11.3 \mu\text{m}$  PAH feature they will be ionized and/or dissociated at different rates. The  $7.7 \mu\text{m}$  PAH feature originates from smaller grains that may be destroyed easier than the bigger grains that emit the  $11.3 \mu\text{m}$  PAH feature.

We suggest the same explanation here although we think the location of silicates, PAHs, and  $\text{H}_2$  relative to the AGN/SF regions may also play a role. As pointed out by [Zakamska \(2010\)](#); [Lambrides et al. \(2019\)](#) the ratio of the  $11.3$  to  $7.7 \mu\text{m}$  PAH features is inversely proportional to the silicate strengths at  $9.7 \mu\text{m}$  but not at all correlated with any of the  $\text{H}_2$  properties (temperature, intensity,  $\text{H}_2/\text{PAH}$ ). [Zakamska \(2010\)](#) suggest that the connection between the silicate strengths and the PAHs emission line ratios can be explained if the PAHs are located behind silicates and water ices in AGN dominated galaxies. A wider range of  $11.3$  to  $7.7 \mu\text{m}$  PAH features ratios measured in AGN hosts may suggest that AGN hosts have more complex and diverse dust geometries than galaxies that do not host AGN.

In figure 3 we compare the distributions of silicate strengths measurements in AGN and non-AGN hosts. We also compare the distributions of silicate strengths measurements in mergers and non-mergers. We find that the silicate strengths of non-AGN hosts differ significantly from those of AGN hosts. The median silicate strengths of AGN are about 3 times lower than those of non-AGN hosts and also span a wider range of values. This matches the finding of [Lambrides et al. \(2019\)](#) for a sample spanning a larger redshift range. The heterogeneous nature of the targets in this study and the preponderance of ( $z < 1$ ) galaxies in our sample may suggest that we miss the most obscured AGN or that in the nearby universe ( $z < 1$ ) the fraction of highly obscured AGN is low ([Lacy et al. 2007](#)).

We also find statistically significant ( $p < 2E - 4$ ) differences between grain size distributions, as estimated by the  $L_{6.2 \mu\text{m}} / L_{7.7 \mu\text{m}}$  between AGN and non-AGN hosts.

### 3.3. Effects of gravitational interactions on the warm molecular gas and dust

We compare the warm molecular gas temperatures of all the mergers in our sample to those of all the non-mergers and find that their median  $\text{H}_2$  S(3) to S(1) ratios are similar, but their distributions are different (the p-value for this comparison are  $5E-6$  and  $2E-6$ ). However, the differences in terms of the warm molecular gas temperatures among AGN only (AGN mergers vs AGN non-mergers) are not highly significant (p-values  $\sim 0.03$ ) and they are non-existent among non-AGN hosts (p values  $\sim 0.9$ ). Among AGN+SF composites we do find slightly more statistically significant differences between mergers and non-mergers (p values  $\sim 0.01$ ).

We also find that the distribution of PAH emission features flux ratios seems to differ significantly between mergers and non-mergers but the statistical strength of those differences decreases sharply when we compare sub-samples: AGN mergers vs AGN non-mergers or SF-mergers vs SF non-mergers. The mergers in our sample have deeper absorption features than non-mergers or early-mergers for both AGN and non-AGN hosts. In a future paper we will analyze the

morphologies of the complete sample from [Lambrides et al. \(2019\)](#) to increase the number of galaxies available for analysis, and assess if/how stellar versus ISM mass may affect our findings.

#### 4. DISCUSSION

In this work we analyze the morphologies and warm ISM properties, as estimated from *griz* imaging with Pan-STARRS and MIR spectroscopic features, of 630 galaxies at  $z < 0.1$ . We use non-parametric two sample tests for censored data as implemented in the R statistical software package *asurv* to compare galaxies that host AGN to those that appear not to host AGN. We use the same tests to compare galaxies whose morphological features suggest they are interacting with other galaxies (mergers) to galaxies that do not seem to have been gravitationally disturbed (non-mergers). The detailed results of these statistical tests are provided in Tables 2 and 3. Here we provide a qualitative summary of our findings and we speculate about their meaning.

- Galaxies that can be identified as AGN on the basis of their MIR properties are statistically different than those that cannot be identified as AGN. In particular, galaxies that host AGN have higher  $H_2/11.3\ \mu m$  PAH ratios and higher  $H_2$  temperature as estimated from the  $H_2\ S(3)/S(1)$  emission-line ratios.
- The MIR emitting dust also appears affected by the presence of an AGN. We find statistically significant differences between the  $11.3\ \mu m$  PAH /  $7.7\ \mu m$  PAH feature ratios of AGN and non-AGN hosts.
- We find statistically significant differences between grain size distributions, as estimated by the  $6.2\ \mu m$  to  $7.7\ \mu m$  PAH feature ratios between AGN and non-AGN hosts.
- We find statistically significant differences between the distributions of silicate strengths in AGN and non-AGN hosts: non-AGN hosts appear to have deeper absorption than AGN-hosts.
- We find some statistical suggestive differences between the  $H_2/11.3\ \mu m$  PAH ratios and  $H_2$  temperature estimated from the  $H_2\ S(3)/S(1)$  emission-line ratios of mergers and non-mergers. However, those differences are less statistically significant than those between AGN and non-AGN hosts.

Our results likely reflect the heterogenous nature of our sample and we may miss the most obscured AGN because in the nearby universe ( $z < 1$ ) the fraction of highly obscured AGN is low ([Lacy et al. 2007](#)). Our results do not establish a relation between the rate of BH growth and the warm ISM. However, we do find highly statistically significant differences between AGN hosts and non-AGN hosts. We do not find differences with the same high statistical significance between mergers and non-mergers.

AGN affect the ISM we measure in the IRS spectra more than gravitational interactions. This is puzzling because there is significant evidence in the literature that mergers trigger AGN and enhance star-formation (e.g. [Ellison et al. 2019](#)). Yet, while we do find statistical differences between the warm  $H_2$  temperatures of mergers and non-mergers, those differences are less significant when we compare AGN merger hosts and AGN non-merger hosts as well as AGN/SF composites.

One speculative explanation is that AGN in mergers were triggered by the merger, and AGNs in non-merger were triggered by secular processes. This would simply mean that the mechanisms that fuel the AGN do not fundamentally alter the ISM on kpc scales. Instead, if an AGN is present it will warm up the MIR-emitting ISM in the central kpc irrelevant of its triggering mechanism, or merger-history.

One alternative possibility to AGN impacting the host galaxy, is that the shock heating we see in the AGN hosts' warm ISM occurs on the same time-scale as the AGN but that it is not directly linked to the AGN itself. It may be possible that the mechanisms which move gas from kiloparsec to subparsec scales (e.g. supernovae, star-formation, galactic bars) also heat up the ISM. Such processes do not lead to the fast shocks measured in some mergers ([Appleton et al. 2006](#), e.g.) but slower shocks and turbulence can enhance the temperature of the warm-molecular gas and the ratio of  $H_2$  emission relative to other coolants (e.g.  $11.3\ \mu m$  PAH emission). We note also that AGN timescales are on the order of  $10^5$  years (e.g. [Schawinski et al. 2015](#)) while our ability to identify mergers is on the order of  $10^6$  (e.g. [Ellison et al. 2019](#)), so if the time-scales for shocked  $H_2$  gas are similar to those of AGN then the statistics of shocked  $H_2$  gas should change with AGN triggering mechanism because different AGN triggering could lead to different gas motions and properties.

[Riffel et al. \(2020\)](#) use SDSS optical spectra for a subsample of the [Lambrides et al. \(2019\)](#) galaxies to suggest that excess of MIR  $H_2$  emission seen in AGN is produced by shocks due to AGN driven outflows in the same clouds that



produce [OI] emission. Spatially resolved kinematics would be required to confirm this hypothesis. Spatially resolved studies of AGN environments in X-rays, radio, and molecular gas such as those performed by [Lanz et al. \(2015\)](#); [Ogle et al. \(2014\)](#); [Appleton et al. \(2018\)](#) with planned and future IR facilities will help us push beyond phenomenological findings to a better physical understanding of the processes that connect AGN and ISM.

*Acknowledgments:* Rebecca Minsley acknowledges support from Research Experience for Undergraduate program at the Institute for Astronomy, University of Hawaii-Manoa funded through NSF grant 6104374 and would like to thank the Institute for Astronomy for their kind hospitality during the course of this project. This research has made use of the NASA/ IPAC Infrared Science Archive, which is operated by the Jet Propulsion Laboratory, California Institute of Technology, under contract with the National Aeronautics and Space Administration.

## REFERENCES

- Allamandola L. J., Hudgens D. M., Sandford S. A., 1999, [ApJL](#), **511**, L115
- Appleton P. N., et al., 2006, [ApJL](#), **639**, L51
- Appleton P. N., et al., 2018, [ApJ](#), **869**, 61
- Armus L., et al., 2007, [ApJ](#), **656**, 148
- Bally J., Lane A. P., 1982, [ApJ](#), **257**, 612
- Becker R. H., White R. L., Helfand D. J., 1994, in Crabtree D. R., Hanisch R. J., Barnes J., eds, *Astronomical Society of the Pacific Conference Series Vol. 61, Astronomical Data Analysis Software and Systems III*. p. 165
- Blumenthal K. A., et al., 2020, [MNRAS](#), **492**, 2075
- Bridge C. R., Carlberg R. G., Sullivan M., 2010, [ApJ](#), **709**, 1067
- Chiaberge M., Gilli R., Lotz J. M., Norman C., 2015, [ApJ](#), **806**, 147
- Diamond-Stanic A. M., Rieke G. H., 2012, [ApJ](#), **746**, 168
- Díaz-Santos T., et al., 2010, [ApJ](#), **723**, 993
- Draine B. T., Li A., 2007, [ApJ](#), **657**, 810
- Ellison S. L., Viswanathan A., Patton D. R., Bottrell C., McConnachie A. W., Gwyn S., Cuillandre J.-C., 2019, [MNRAS](#), **487**, 2491
- Feigelson E. D., Nelson P. I., 1985, [ApJ](#), **293**, 192
- Gautier III T. N., Fink U., Larson H. P., Treffers R. R., 1976, [ApJL](#), **207**, L129
- Genzel R., et al., 1998, [ApJ](#), **498**, 579
- Guillard P., Boulanger F., Pineau Des Forêts G., Appleton P. N., 2009, [A&A](#), **502**, 515
- Guillard P., et al., 2012, [ApJ](#), **749**, 158
- Hill M. J., Zakamska N. L., 2014, [MNRAS](#), **439**, 2701
- Hopkins P. F., Richards G. T., Hernquist L., 2007, [ApJ](#), **654**, 731
- Hopkins P. F., Torrey P., Faucher-Giguère C.-A., Quataert E., Murray N., 2016, [MNRAS](#), **458**, 816
- Houck J. R., et al., 2004, in Mather J. C., ed., *Society of Photo-Optical Instrumentation Engineers (SPIE) Conference Series Vol. 5487, Proc. SPIE*. pp 62–76, doi:10.1117/12.550517
- Isobe T., Feigelson E. D., Nelson P. I., 1986, [ApJ](#), **306**, 490
- Ivezić Ž., et al., 2002, [AJ](#), **124**, 2364
- Kaplan E., Meier P., 1958, *J. Am. Statistical Associations*, **53**, 457
- Lacy M., Hill G. J., Kaiser M.-E., Rawlings S., 1993, [MNRAS](#), **263**, 707
- Lacy M., Sajina A., Petric A. O., Seymour N., Canalizo G., Ridgway S. E., Armus L., Storrie-Lombardi L. J., 2007, [ApJL](#), **669**, L61
- Lambrides E. L., Petric A. O., Tchernyshyov K., Zakamska N. L., Watts D. J., 2019, [MNRAS](#), p. 1261
- Lanz L., Ogle P. M., Evans D., Appleton P. N., Guillard P., Emonts B., 2015, [ApJ](#), **801**, 17
- Larkin J. E., Armus L., Knop R. A., Soifer B. T., Matthews K., 1998, [ApJS](#), **114**, 59
- Larson K. L., et al., 2016, [ApJ](#), **825**, 128
- Lebouteiller V., Barry D. J., Spoon H. W. W., Bernard-Salas J., Sloan G. C., Houck J. R., Weedman D. W., 2011, *The Astrophysical Journal Supplement Series*, **196**, 8
- Li A., Draine B. T., 2001, [ApJ](#), **554**, 778
- Moorwood A. F. M., Oliva E., 1988, [A&A](#), **203**, 278
- Nair P. B., Abraham R. G., 2010, [ApJS](#), **186**, 427
- Nesvadba N. P. H., Boulanger F., Lehnert M. D., Guillard P., Salome P., 2011, [A&A](#), **536**, L5
- Ogle P., Antonucci R., Appleton P. N., Whysong D., 2007, [ApJ](#), **668**, 699
- Ogle P. M., Lanz L., Appleton P. N., 2014, [ApJL](#), **788**, L33
- Petric A. O., et al., 2011, [ApJ](#), **730**, 28
- Petric A. O., et al., 2018, *The Astronomical Journal*, **156**, 295
- Riffel R. A., Zakamska N. L., Riffel R., 2020, [MNRAS](#), **491**, 1518
- Rigopoulou D., Kunze D., Lutz D., Genzel R., Moorwood A. F. M., 2002, [A&A](#), **389**, 374
- Roussel H., et al., 2007, [ApJ](#), **669**, 959

- Schawinski K., Koss M., Berney S., Sartori L. F., 2015, [MNRAS](#), **451**, 2517
- Smith J. D. T., et al., 2007, [PASP](#), **119**, 1133
- Stierwalt S., et al., 2013, [ApJS](#), **206**, 1
- Stierwalt S., et al., 2014, [ApJ](#), **790**, 124
- Werner M. W., et al., 2004, [ApJS](#), **154**, 1
- Zakamska N. L., 2010, [Nature](#), **465**, 60
- Zheng W., Kriss G. A., Telfer R. C., Grimes J. P., Davidsen A. F., 1997, [ApJ](#), **475**, 469